

Phonon-assisted Kondo Effect in a Single-Molecule Transistor out of Equilibrium

Zuo-Zi Chen,^{1,*} Haizhou Lu,¹ Rong Lü,¹ and Bang-fen Zhu^{1,2,†}

¹*Center for Advanced Study, Tsinghua University, Beijing 100084, P. R. China*

²*Department of Physics, Tsinghua University, Beijing 100084, P. R. China*

(Dated: December 2, 2024)

The Kondo effect in the single-molecule transistor is studied in the presence of the localized electron-vibration-mode interaction, finite bias voltage and Zeeman splitting. With the improved technique for the electron-phonon system and the extended equation-of-motion approach, the phonon-Kondo satellites with various shapes in the spectral function and differential conductance are fully confirmed, demonstrating two types of Kondo-phonon satellites associated with spin singlets respectively formed by electron and hole states. Moreover, these peculiar signatures of satellites can be traced in the differential conductance, and are entirely resolved in the spin-polarized spectral functions in the presence of finite Zeeman splitting. A clear physical picture is presented to explain the formation of these Kondo-phonon satellites.

PACS numbers: 72.15.Qm, 85.65.+h, 73.63.Kv, 71.38.-k

The Kondo effect as a manifestation of strongly correlations between electrons has been extensively studied in the content of quantum dot physics in past years[1, 2]. Recently, its realization in the single-molecule transistor (SMT) has attracted a lot of attentions[3, 4], in particular the reported inelastic electron tunneling in the Kondo regime[5] owing to the molecular vibrational feature of the SMT [6, 7]. This has stimulated subsequent efforts to investigate the interplay of the electron-phonon interaction (EPI) and the Kondo correlation in the transport properties of the SMT theoretically, such as using the numerical renormalization group[8], Schrieffer-Wolff transformation[9], and slave-boson approaches[10]. However, most of these researches are focused on the dressing effect owing to the EPI, and little has discussed whether and how the Kondo phonon-satellite structure develops, especially in the presence of the finite bias voltage and Zeeman splitting.

It is known that, without the Coulomb interaction, the phonon satellites are sensitive to the Fermi levels at leads as well as the dot level[11]. When the temperature is too low to excite phonons thermally, the phonon satellites can only be developed below (above) the resonant level if this level is occupied (empty) initially, as electrons can then emit phonons only. On the other hand, in the Kondo regime, two collective spin singlet states will be formed between the localized state and the excited electron states above the Fermi level μ or the excited hole states below μ because of spin exchange processes[13], which together contribute to the sharp Kondo peak pinning at the Fermi surface in the local density of states. Note that both the EPI effect and the Kondo effect are sensitive to the Fermi surface, thus interesting physics resulting from their interplay are expected.

In this Letter, with the Anderson-Holstein Hamiltonian we study the joint effects of the Kondo correlation, electron-phonon interaction and Zeeman splitting on the nonequilibrium transport properties through a

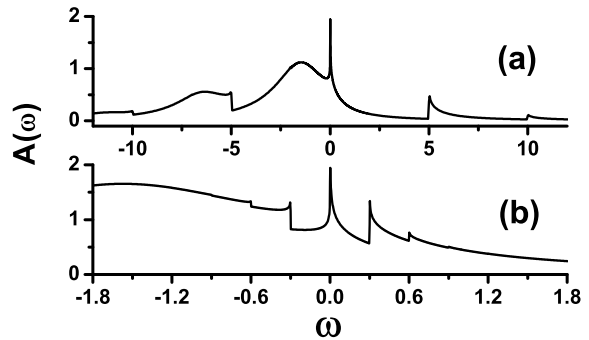


FIG. 1: The spectral function for spin-degenerate local electrons, A , as functions of ω in unit of Γ , where $\mu_L = \mu_R = 0$, $\bar{\epsilon}_0 = -2.5\Gamma$, $g = 0.4\Gamma$, $k_B T = 0.0002\Gamma$, and (a) $\hbar\omega_0 = 5.0\Gamma$, and (b) $\hbar\omega_0 = 0.3\Gamma$.

SMT by using the improved nonperturbative canonical transformation for the EPI[11] and the extended equation-of-motion (EOM) approach, which is good at treating the non-equilibrium situation, as well as the finite Zeeman splitting[12]. With these improved techniques, it has been found that (i) The phonon-satellites around the Kondo main peak exhibit quite different spectral shapes (Fig.1) and also manifest themselves in the non-equilibrium transport; (ii) Two types of spin exchange processes, associated with the collective spin singlets formed by electron states and by hole states respectively, can be clearly distinguished in the Kondo satellites; and (iii) With a finite Zeeman splitting larger than the Kondo temperature, for a given spin, its Kondo-phonon satellites only appear on one side of the main Kondo peak in the spin-resolved spectral function, and on the opposite side for the opposite spin component.

The physical picture for the Kondo phonon-satellites in the SMT can be understood as follows. As shown

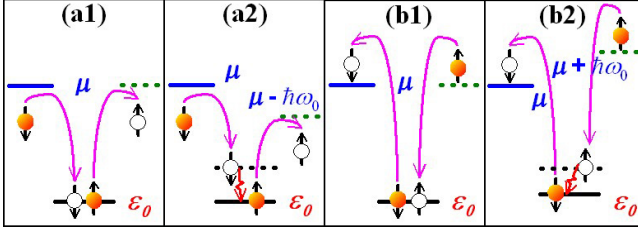


FIG. 2: (color online) Schematic illustration for the spin exchange processes associated with the formation of the Kondo satellites.

in Fig.2(a1), a localized hole state in a SMT exchanges with the excited holes below the Fermi energy at leads μ to form a Kondo spin-singlet. When an electron hops to the localized state by emitting a phonon, as shown in Fig.2(a2), only the holes with energy below $\mu - \hbar\omega_0$ exchange with the localized hole because of the requirement of the energy conservation. Thus a phonon-satellite pinning at $\mu - \hbar\omega_0$ appears in the density of states or tunneling spectra. Similarly, a spin-singlet consisting of a localized SMT electron and excited electrons above μ is depicted in Fig.2(b1), and only the electrons above $\mu + \hbar\omega_0$ can exchange with the local electron if the hopping processes are accompanied by emitting a phonon as shown in Fig.2(b2), which will give rise to the satellite pinning at $\mu + \hbar\omega_0$. That means although both the processes shown in Fig.2(a1) and (b1) contribute to the main Kondo peak, they can be distinguished by their Kondo satellites. In other words, the contribution of each type of exchange processes to the main Kondo peak can in principle be picked out by comparing with the satellites on each sides of the main peak.

The Anderson-Holstein Hamiltonian, describing the SMT as a single localized state coupled linearly to one local vibration mode and to the left (L) and right (R) non-interacting leads, reads

$$\mathbf{H} = \sum_{\alpha; \mathbf{k}, \sigma} \varepsilon_{\alpha \mathbf{k}} \mathbf{c}_{\alpha \mathbf{k} \sigma}^\dagger \mathbf{c}_{\alpha \mathbf{k} \sigma} + \sum_{\sigma} \varepsilon_{\sigma} \mathbf{n}_{\sigma} + U_0 \mathbf{n}_{\uparrow} \mathbf{n}_{\downarrow} + \hbar \omega_0 \mathbf{a}^\dagger \mathbf{a} + \sum_{\sigma} \lambda \mathbf{n}_{\sigma} (\mathbf{a}^\dagger + \mathbf{a}) + \sum_{\alpha; \mathbf{k}, \sigma} (V_{\alpha \mathbf{k}} \mathbf{c}_{\alpha \mathbf{k} \sigma}^\dagger \mathbf{d}_{\sigma} + h.c.), \quad (1)$$

where $\mathbf{c}_{\alpha \mathbf{k} \sigma}^\dagger (\mathbf{c}_{\alpha \mathbf{k} \sigma})$ and $\mathbf{d}_{\sigma}^\dagger (\mathbf{d}_{\sigma})$ are the creation (annihilation) operators for the conduction electron with energy $\varepsilon_{\alpha \mathbf{k}}$ and the localized SMT electron with energy ε_{σ} , respectively, $\mathbf{n}_{\sigma} = \mathbf{d}_{\sigma}^\dagger \mathbf{d}_{\sigma}$, U_0 is the on-site Coulomb repulsion, σ denotes the spin index and $\alpha = L, R$. The operator \mathbf{a}^\dagger (\mathbf{a}) creates (annihilates) the local vibration mode with frequency ω_0 , λ is the EPI strength, $V_{\alpha \mathbf{k}}$ is the tunneling coupling between the localized and lead electrons, which results in a level broadening $\Gamma = (\Gamma_L + \Gamma_R)/2$, where $\Gamma_{\alpha}(\omega) \equiv 2\pi \sum_{\mathbf{k}} |V_{\alpha \mathbf{k}}|^2 \delta(\omega - \varepsilon_{\alpha \mathbf{k}})$.

To treat the EPI non-perturbatively, we introduce a canonical transformation, $\mathbf{S} = \frac{\lambda}{\omega_0} \sum_{\sigma} \mathbf{n}_{\sigma} (\mathbf{a}^\dagger - \mathbf{a})$, then

the Hamiltonian is transformed into $\bar{\mathbf{H}} \equiv e^{\mathbf{S}} \mathbf{H} e^{-\mathbf{S}} = \bar{\mathbf{H}}_{\text{ph}} + \bar{\mathbf{H}}_{\text{el}}$, where the phonon part $\bar{\mathbf{H}}_{\text{ph}} = \hbar \omega_0 \mathbf{a}^\dagger \mathbf{a}$, and the electron part turns out to be the Anderson Hamiltonian, namely

$$\begin{aligned} \bar{\mathbf{H}}_{\text{el}} = & \sum_{\alpha, \mathbf{k}, \sigma} \varepsilon_{\alpha \mathbf{k}} \mathbf{c}_{\alpha \mathbf{k} \sigma}^\dagger \mathbf{c}_{\alpha \mathbf{k} \sigma} + \sum_{\sigma} \bar{\varepsilon}_{\sigma} \mathbf{n}_{\sigma} + \bar{U}_0 \mathbf{n}_{\uparrow} \mathbf{n}_{\downarrow} \\ & + \sum_{\alpha, \mathbf{k}, \sigma} (\bar{V}_{\alpha \mathbf{k}} \mathbf{c}_{\alpha \mathbf{k} \sigma}^\dagger \mathbf{d}_{\sigma} + h.c.). \end{aligned} \quad (2)$$

The parameters with bar in Eq.(2) correspond to the renormalized ones owing to the transformation, e.g., the SMT level is shifted to $\bar{\varepsilon}_{\sigma} = \varepsilon_{\sigma} - g\omega_0$ with $g \equiv (\lambda/\omega_0)^2$, and the on-site repulsion is renormalized to $\bar{U}_0 = U_0 - 2g\omega_0$, which may even become negative for strong EPI[8], but here we limit ourselves to the case of the positive \bar{U}_0 only. Besides, $\bar{V}_{\alpha \mathbf{k}} \equiv V_{\alpha \mathbf{k}} \mathbf{X}$, and $\bar{\Gamma} = \Gamma \mathbf{X}^\dagger \mathbf{X}$ with $\mathbf{X} \equiv \exp [-(\lambda/\omega_0) (\mathbf{a}^\dagger - \mathbf{a})]$, indicating that hybridizations between the local electron and conduction electrons are modulated by local phonons. In the present work, only the weak tunneling coupling case is considered, then the operator \mathbf{X} can be approximated by its expectation value at thermal equilibrium, $\langle \mathbf{X} \rangle = \exp [-g(N_{\text{ph}} + 1/2)]$, with N_{ph} defined as the population of phonons at temperature T [11, 14].

With the approximations above, the transformed Hamiltonian is decoupled. Within this framework, the lesser Green function can be rigorously separated into the electron part and phonon part,

$$\begin{aligned} G_{\sigma}^<(t) & \equiv i \langle \mathbf{d}_{\sigma}^\dagger(0) \mathbf{d}_{\sigma}(t) \rangle = i \langle \bar{\mathbf{d}}_{\sigma}^\dagger e^{i \bar{\mathbf{H}} t} \bar{\mathbf{d}}_{\sigma} e^{-i \bar{\mathbf{H}} t} \rangle \\ & = i \langle \mathbf{d}_{\sigma}^\dagger e^{i \bar{\mathbf{H}}_{\text{el}} t} \mathbf{d}_{\sigma} e^{-i \bar{\mathbf{H}}_{\text{el}} t} \rangle_{\text{el}} \langle \mathbf{X}^\dagger e^{i \bar{\mathbf{H}}_{\text{ph}} t} \mathbf{X} e^{-i \bar{\mathbf{H}}_{\text{ph}} t} \rangle_{\text{ph}} \\ & = \sum_{n=-\infty}^{\infty} L_n \bar{G}_{\sigma}^<(\omega + n\omega_0), \end{aligned} \quad (3)$$

and similarly the greater Green function is formulated as

$$G_{\sigma}^>(\omega) = \sum_{n=-\infty}^{\infty} L_n \bar{G}_{\sigma}^>(\omega - n\omega_0), \quad (4)$$

where $\bar{G}_{\sigma}^>(<)$ is the dressed Green function associated with $\bar{\mathbf{H}}_{\text{el}}$, and

$$L_n = e^{-g(2N_{\text{ph}}+1)} e^{n\omega_0/2k_B T} I_n \left(2g \sqrt{N_{\text{ph}}(N_{\text{ph}}+1)} \right), \quad (5)$$

with $I_n(z)$ the n -th Bessel function of complex argument. The spectral function is then calculated with the lesser and greater Green functions via $A_{\sigma}(\omega) = i(G_{\sigma}^>(\omega) - G_{\sigma}^<(\omega))$. It should be emphasized that people usually evaluate the spectral function via $A_{\sigma}(\omega) = i(G_{\sigma}^r(\omega) - G_{\sigma}^a(\omega))$,[7] in which the retarded and advanced Green functions, G_{σ}^r and G_{σ}^a , are approximately separated into the electron and phonon parts by ignoring the

difference between the N_{ph} and $N_{ph}+1$, which works only in the high-temperature limit. However, the phonon-Kondo problem studied here is certainly not the case, as the characteristic Kondo temperature, T_K , is very low. Hence the prescription we have recently presented may be more appropriate[11].

Within the Keldysh formulism, the dressed Green functions $\bar{G}_\sigma^{>(<)}$ can be derived from $\bar{\mathbf{H}}_{el}$ with the help of EOM approach. Since the usual approximation in decoupling the higher-order Green functions generated by EOM is only valid nearby or above the Kondo tempera-

ture T_K [12], we extend the decoupling scheme developed by Lacroix[15] to finite \bar{U}_0 , finite Zeeman splitting, and non-equilibrium cases in order to treat the Kondo resonance more accurately at the low temperature and non-equilibrium. Hence, the usually ignored higher-order retarded Green function, for example $\langle\langle\mathbf{d}_\sigma\mathbf{c}_{\alpha\mathbf{k}\bar{\sigma}}^\dagger\mathbf{c}_{\alpha'\mathbf{k}'\sigma},\mathbf{d}_\sigma^\dagger\rangle\rangle$, is now approximated as $\langle\mathbf{d}_\sigma\mathbf{c}_{\alpha\mathbf{k}\bar{\sigma}}^\dagger\rangle\langle\langle\mathbf{c}_{\alpha'\mathbf{k}'\sigma},\mathbf{d}_\sigma^\dagger\rangle\rangle$, and the matrix element $\langle\mathbf{d}_\sigma\mathbf{c}_{\alpha\mathbf{k}\bar{\sigma}}^\dagger\rangle$ is determined self-consistently. The retarded Green function turns out to be

$$\bar{G}_\sigma^r(\omega) = \frac{1 - (\langle\bar{\mathbf{n}}_\sigma\rangle + \bar{P}_\sigma(\bar{\omega}_\sigma^0) + \bar{P}_\sigma^*(-\bar{\omega}^U))}{\omega - \bar{\varepsilon}_\sigma - \bar{\Sigma}^{(T)}(\omega) + \frac{\bar{U}_0\bar{\Sigma}_\sigma^{(1)}(\omega)}{\omega - \bar{\varepsilon}_\sigma - \bar{U}_0 - \bar{\Sigma}^{(T)}(\omega) - \bar{\Sigma}_\sigma^{(3)}(\omega)}} + \frac{\langle\bar{\mathbf{n}}_\sigma\rangle + \bar{P}_\sigma(\bar{\omega}_\sigma^0) + \bar{P}_\sigma^*(-\bar{\omega}^U)}{\omega - \bar{\varepsilon}_\sigma - \bar{U}_0 - \bar{\Sigma}^{(T)}(\omega) - \frac{\bar{U}_0\bar{\Sigma}_\sigma^{(2)}(\omega)}{\omega - \bar{\varepsilon}_\sigma - \bar{\Sigma}^{(T)}(\omega) - \bar{\Sigma}_\sigma^{(3)}(\omega)}}, \quad (6)$$

where $\bar{\omega}_\sigma^0 \equiv \omega + \bar{\varepsilon}_\sigma - \bar{\varepsilon}_\sigma$, $\bar{\omega}^U \equiv \omega - \bar{\varepsilon}_\sigma - \bar{\varepsilon}_\sigma - \bar{U}_0$, and the correlation function between SMT and leads commonly neglected, $\bar{P}_\sigma(\omega)$ is defined as $\sum_{\alpha\mathbf{k}} \bar{V}_{\alpha\mathbf{k}}^* \langle\mathbf{d}_\sigma^\dagger \mathbf{c}_{\alpha\mathbf{k}\bar{\sigma}}\rangle g_{\alpha\mathbf{k}}^r(\omega)$, in which $g_{\alpha\mathbf{k}}^r(\omega)$ is the unperturbed retarded Green function of the lead electron. The self-energy associated with the resonant tunneling processes, $\bar{\Sigma}^{(T)}(\omega)$, is defined as $\sum_{\alpha\mathbf{k}} |\bar{V}_{\alpha\mathbf{k}}|^2 g_{\alpha\mathbf{k}}^r(\omega)$, and self-energies related to the Kondo correlation are explicitly expressed as $\bar{\Sigma}_\sigma^{(3)}(\omega) = \bar{\Sigma}^{(T)}(\bar{\omega}_\sigma^0) - (\bar{\Sigma}^{(T)}(-\bar{\omega}^U))^*$, $\bar{\Sigma}_\sigma^{(1)}(\omega) = \bar{\Sigma}_\sigma^{(0)}(\omega) - \bar{\Sigma}^{(T)}(\omega) [\bar{P}_\sigma(\bar{\omega}_\sigma^0) + \bar{P}_\sigma^*(-\bar{\omega}^U)]$, $\bar{\Sigma}_\sigma^{(2)} = \bar{\Sigma}_\sigma^{(3)} - \bar{\Sigma}_\sigma^{(1)}$, and $\bar{\Sigma}_\sigma^{(0)}(\omega) = \bar{B}_\sigma(\omega) + [\bar{F}_\sigma(\bar{\omega}_\sigma^0) - \bar{F}_\sigma^*(-\bar{\omega}^U)]$, where $\bar{B}_\sigma(\omega) = -2i\text{Im}\{\sum_{\alpha'\mathbf{k}'} \bar{V}_{\alpha'\mathbf{k}'}^* \langle\mathbf{d}_\sigma^\dagger \mathbf{c}_{\alpha'\mathbf{k}'\bar{\sigma}}\rangle\} [\sum_{\alpha\mathbf{k}} |\bar{V}_{\alpha\mathbf{k}}|^2 (g_{\alpha\mathbf{k}}^r(\omega))^2]$ and $\bar{F}_\sigma(\omega) = \sum_{\alpha\mathbf{k},\alpha'\mathbf{k}'} \bar{V}_{\alpha\mathbf{k}}^* \bar{V}_{\alpha'\mathbf{k}'} \langle\mathbf{c}_{\alpha'\mathbf{k}'\bar{\sigma}}^\dagger \mathbf{c}_{\alpha\mathbf{k}\bar{\sigma}}\rangle g_{\alpha\mathbf{k}}^r(\omega)$. In the wide-band limit, $\bar{\Sigma}^{(T)}(\omega) \approx -i\bar{\Gamma}$, and $\bar{\Sigma}_\sigma^{(0)}(\omega) \approx \sum_\alpha \frac{\bar{\Gamma}_\alpha}{2\pi} [\psi\left(\frac{1}{2} + \frac{\bar{\omega}^U + \mu_\alpha}{i2\pi k_B T}\right) - \psi\left(\frac{1}{2} + \frac{\bar{\omega}_\sigma^0 - \mu_\alpha}{i2\pi k_B T}\right) - i\pi]$, where the Psi function ψ is the logarithmic derivative of gamma function. Now, the self-consistent equation for $\bar{P}_\sigma(\omega)$ can be simplified as

$$\bar{P}_\sigma(\omega) = \int \frac{d\omega'}{2\pi} \frac{[\bar{\Gamma}_L f_L(\omega') + \bar{\Gamma}_R f_R(\omega')] \bar{G}_\sigma^{r*}(\omega')}{\omega - \omega' + i0^+}, \quad (7)$$

which, together with Eq.(6), gives the dressed retarded Green function \bar{G}_σ^r . Finally, by the Keldysh formulas $\bar{G}_\sigma^{>(<)} = \bar{G}_\sigma^r \bar{\Sigma}_\sigma^{>(<)} \bar{G}_\sigma^a$, in which the the greater (lesser) self-energies are evaluated by the ansatz adopted by Ng[17], the dressed greater and lesser Green functions are obtained as

$$\begin{aligned} \bar{G}_\sigma^>(\omega) &= i([\bar{\Gamma}_L(1 - f_L(\omega)) + \bar{\Gamma}_R(1 - f_R(\omega))] \text{Im}\bar{G}_\sigma^r(\omega)/\bar{\Gamma}), \\ \bar{G}_\sigma^<(\omega) &= -i[\bar{\Gamma}_L f_L(\omega) + \bar{\Gamma}_R f_R(\omega)] \text{Im}\bar{G}_\sigma^r(\omega)/\bar{\Gamma}. \end{aligned} \quad (8)$$

Substituting Eq.(8) into Eqs.(3),and (4), one can obtain the greater (lesser) Green function and subsequently the

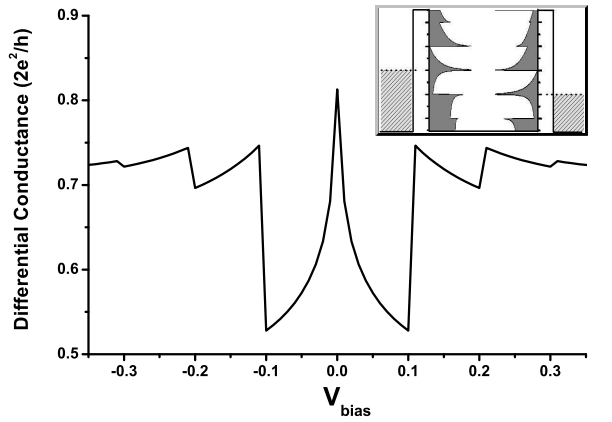


FIG. 3: The differential conductance as a function of the bias voltage. Here $\bar{\varepsilon}_\uparrow = \bar{\varepsilon}_\downarrow = -2.5\Gamma$, $g = 0.5\Gamma$, $k_B T = 0.0002\Gamma$, and $\hbar\omega_0 = 0.1\Gamma$. As an example, the origin of the first phonon peak is schematically illustrated in the inset.

spectral function of SMT as plotted in Fig.1. It is worthy to point out that these calculations are valid even when the system is driven out of equilibrium by a finite bias voltage, which allows us to calculate the non-equilibrium transport properties.

With the current through the SMT region as[16] $J = \sum_\sigma \frac{ie}{2h} \int d\omega \{[f_L(\omega)\Gamma_L - f_R(\omega)\Gamma_R]A_\sigma(\omega) + (\Gamma_L - \Gamma_R)G_\sigma^<(\omega)\}$, the differential conductance is evaluated by $G = \partial J / \partial V_{bias}$. As shown in Fig.3, the differential conductance exhibits zero-bias anomaly at low temperature, which is viewed as the experimental evidence for the Kondo effect in the quantum dot. In the finite bias case, the main Kondo peak in the spectral function is split into two peaks pinning at each Fermi level [12],

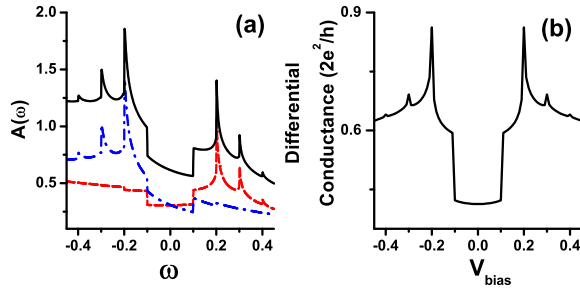


FIG. 4: (color online) (a) The total (solid line) and spin-resolved (dashed line for spin up, dot-dash line for spin down) spectral functions, and (b) the differential conductance in the presence of finite Zeeman splitting[18]. Here $\bar{\epsilon}_0 = -2.5\Gamma$, $g = 0.4\Gamma$, $k_B T = 0.0002\Gamma$, $\Delta = 0.2\Gamma$ and $\hbar\omega_0 = 0.1\Gamma$.

and the phonon satellites are also split into two subsets. As demonstrated in the inset of Fig.3, each time a satellite matches one of the Fermi surfaces, the differential conductance will be peaked. In other words, a set of phonon peaks appear in the differential conductance spectra when $V_{\text{bias}} = n\hbar\omega_0$, which has been observed in a very recent experiment[5] as an experimental evidence for the phonon-assisted Kondo effect.

Now, it is easy to generalize the above investigations to the case of finite Zeeman splitting, where a local magnetic field induces the energy level splitting of the localized electron state, i.e. $\epsilon_{\uparrow} = \epsilon_0 + \Delta/2$ and $\epsilon_{\downarrow} = \epsilon_0 - \Delta/2$. In the absence of the EPI, it is known that the Kondo peak in $A_{\uparrow}(\omega)$ ($A_{\downarrow}(\omega)$) is shifted from μ by Δ ($-\Delta$). In the presence of EPI, the satellite structure will be developed as shown in Fig.4(a). It is interesting to notice that only the satellites below (above) the main peak appear in $A_{\uparrow}(\omega)$ ($A_{\downarrow}(\omega)$) when the Zeeman splitting Δ is much larger than the Kondo temperature $k_B T_K$. Since satellites on the other side are associated with different spin exchange processes, the results indicate that the dominant contribution to the main peak in $A_{\uparrow}(\omega)$ comes from the coupling of the local state with the excited conduction electron states, while for $A_{\downarrow}(\omega)$ the dominant contribution comes from the coupling with the excited hole states. This distinct feature comes from the interplay between the EPI and Kondo effect at larger Zeeman splitting, and can be observed by measuring the differential conductance. As shown in Fig.4(b), there is no satellite appearing in the regime $\mu - \Delta < V_{\text{bias}} < \mu + \Delta$.

In summary, taking advantage of our improved treatment of the electron-phonon interaction, combined with the extended equation of motion approach, we have investigated the Kondo effect in the SMT in the presence of the electron-phonon interaction, finite bias voltage, and larger Zeeman splitting. The peculiar phonon-Kondo satellites in the spectral function as well as differential conductance have been found, with a clear physical ex-

planation on the formation of these satellites presented.

The authors thank the helpful discussions with H. Zhai, Z. G. Zhu, F. Ye, C. X. Liu and R. B. Liu. This work is supported by the NSF of China (Grant No. 10374056), the MOE of China (Grant No. 2002003089 and No. 200221), and the Program of Basic Research Development of China (Grant No. 2001CB610508).

* Electronic address: zzchen@castu.tsinghua.edu.cn

† Electronic address: bfzhu@castu.tsinghua.edu.cn

- [1] T. K. Ng and P. A. Lee, Phys. Rev. Lett. **61**, 1768 (1988); L. I. Glazman and M. E. Raikh, JETP Lett. **47**, 452 (1988).
- [2] S. M. Cronenwett, et al., Science **281**, 540 (1998); D. G. Gordon, et al., Nature (London) **391**, 156 (1998); J. Schmid, et al., Physica B (Amsterdam) **256**, 182, (1998); W. G. v. d. Wiel, et al., Science **289**, 22 (2000).
- [3] J. Park, et al., Nature (London) **417**, 722 (2002); W. Liang, et al., Nature (London) **417**, 725 (2002); A. N. Pasupathy, et. al., Science **306**, 86 (2004); A. Kogan, et al., Science, **304**, 1293 (2004).
- [4] M. S. Choi, et. al., Phys. Rev. Lett. **92**, 056601 (2004); J. Martinek, et. al., Phys. Rev. Lett. **91**, 127203 (2003).
- [5] L.H. Yu and D. Natelson, Nano Letters **4**, 79 (2004); Nanotechnology **15**, S517 (2004); L. H. Yu, et al., Phys. Rev. Lett. **93**, 266802 (2004).
- [6] H. Park, et al., Nature (London) **407**, 57 (2000); J. Koch and F. V. Oppen, cond-mat/0409667; M. Galperin, et al., Nano Letters **4**, 1605 (2004).
- [7] J. X. Zhu and A. V. Balatsky, Phys. Rev. B **67**, 165326 (2003); D. M. T. Kuo and Y. C. Chang, Phys. Rev. B **66**, 085311 (2002); U. Lundin and R.H. Mckenzie, Phys. Rev. B **66**, 075303 (2002).
- [8] P.S. Cornaglia, et. al., Phys. Rev. Lett. **93**, 147201 (2004); P.S. Cornaglia, et. al., Phys. Rev. B **71** 075320 (2005); P. S. Cornaglia and D. R. Grempel, cond-mat/0502606.
- [9] J. Paaske and K. Flensberg, cond-mat/0409158.
- [10] H. C. Lee and H. Y. Choi, Phys. Rev. B **70**, 085114 (2004).
- [11] Z. Z. Chen, R. Lü, and B. F. Zhu, Phys. Rev. B **71**, xxxxxx (2005)(cond-mat/0410674).
- [12] Y. Meir and P. A. Lee, Phys. Rev. Lett. **70**, 2601 (1993); R. Świrkowicz, et al., Phys. Rev. B **68**, 195318 (2003).
- [13] K. Yosida, Phys. Rev. **147**, 223 (1966); G. D. Mahan, Many-Particle Physics, P967, 2nd Ed., (Plenum press, New York and London, 1990).
- [14] G. D. Mahan, Many-Particle Physics, P533, 2nd Ed., (Plenum press, New York and London, 1990).
- [15] C. Lacroix, J. Phys. F: Metal Phys. **11**, 2389-97 (1981).
- [16] Y. Meir and N. S. Wingreen, Phys. Rev. Lett. **68**, 2512 (1992); A. -P. Jauho, N. S. Wingreen and Y. Meir, Phys. Rev. B **50**, 5528 (1994).
- [17] T. K. Ng, Phys. Rev. Lett. **76**, 487 (1996).
- [18] The jumps of the spectral functions at $\omega = \pm\omega_0$ originate from the satellites of the resonant peaks, which have the nonvanishing tails near the Fermi surface. Subsequently, the differential conductance also represents two obvious cuts at $V_{\text{bias}} = \pm\hbar\omega_0$.